Electrochemistry and Absorption and Emission Spectroscopy of New Ortho-Metalated Complexes of Rh(III) and Ir(III) with the Ligands 1,4,5,8-Tetraazaphenanthrene and 1,4,5,8,9,12-Hexaazatriphenylene

P. Didier, I. Ortmans, and A. Kirsch-De Mesmaeker[†,*]

Université Libre de Bruxelles, Chimie Organique Physique, CP 160/08, 50 avenue F. D. Roosevelt, 1050 Bruxelles, Belgium

R. J. Watts

Department of Chemistry, University of California, Santa Barbara, California 93106

Received March 23, 1993[⊕]

The electrochemical and UV–visible absorption and emission properties of new heteroleptic ortho-metalated complexes of Rh(III) and Ir(III) are reported and compared to those of similar complexes studied previously in the literature. These novel compounds contain two ortho-metalating ligands (ortho-C-deprotonated forms of 2-phenylpyridine, PPY) and a polyazaaromatic ligand such as 1,4,5,8-tetraazaphenanthrene (TAP) or 1,4,5,8,9,12-hexaazatriphenylene (HAT). The electrochemical behavior, studied by cyclic voltammetry, shows the presence of two reversible reductions, both on a TAP or HAT ligand, and of an irreversible oxidation. Interestingly, contrary to the Rh complexes studied previously in the literature, the TAP- and HAT–Rh compounds present emissions clearly characteristic of distorted CT states to the TAP or HAT ligand, as shown by the unstructured emission spectra at room temperature and 77 K, by their hypsochromic shifts from fluid solutions to rigid glasses at 77 K, and by the luminescence lifetimes. On the basis of these data and due to the irreversible behavior of the oxidation wave, these CT states for Rh complexes are described in terms of σ-bond-to-ligand (Rh–C σ bond) charge-transfer (SBLCT) transitions. The iridium HAT complex, like the other similar Ir complexes examined in the literature, shows a dual emission at 77 K in a frozen glass, indicated by two bands in the luminescence spectrum with two distinct lifetimes. They are discussed as originating from two excited states: one metal-to-ligand charge-transfer state (^{3}MLCT), [Ir^{IV} $HAT^{\bullet-}$]*, and one SBLCT state, both with a charge transfer to the accepting HAT π^* orbital.

Introduction

In order to design new polymetallic compounds, we have investigated the possibility of complexing Ru(II) and, more recently, Rh(III) and Ir(III), to the bridging ligand 1,4,5,8,9,12-hexaazatriphenylene (HAT, I). This latter, with its three

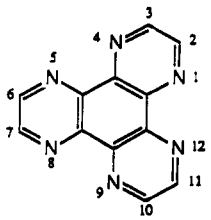

I

symmetrically disposed chelation sites, allows the complexation of up to three transition metal ions. In a first step, polymetallic homonuclear Ru(II) complexes with $Ru(BPY)_2^{2+}$ moieties (BPY = 2,2′-bipyridine) bridged by the HAT ligand have been prepared, yielding the symmetric bi- and trimetallic edifices;[1-4] afterward[4] $Ru(BPY)_2^{2+}$, and $Ru(HAT)_2^{2+}$ moieties have been combined with the bridging HAT to lead to nonsymmetric complexes (TAP = 1,4,5,8-tetraazaphenanthrene).

For complexes with Rh(III) ions, attempts to synthesize mononuclear tris-chelated non-orthometalated compounds with at least one HAT or one TAP ligand remained unsuccessful, whereas with the Ru(II) all the combinations of ligands are possible, leading to a choice of different heteroleptic complexes.[4] It may be possible that the TAP and HAT ligands have too strong a π-deficient character to form stable bonds with a Rh(III), which is already chelated to two BPY or two PHEN (1,10-phenanthroline) ligands.

Therefore we tested a combination of one TAP or one HAT ligand with ortho-metalating ligands such as the ortho-C-deprotonated form of 2-phenylpyridine (PPY), which is known to be a strong σ-donor ligand.[5,6] In this paper it is shown that the dichloro-bridged dimers $[Rh(PPY)_2Cl]_2$ and $[Ir(PPY)_2Cl]_2$ react easily with a TAP or a HAT ligand to form the corresponding monometallic complexes $Rh(PPY)_2TAP^+$ (II), $Rh(PPY)_2HAT^+$ (III), and $Ir(PPY)_2HAT^+$. Their electrochemical and spectro-

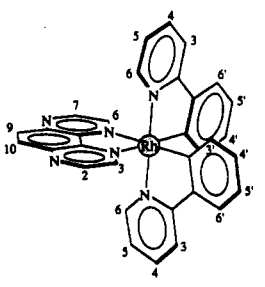

II

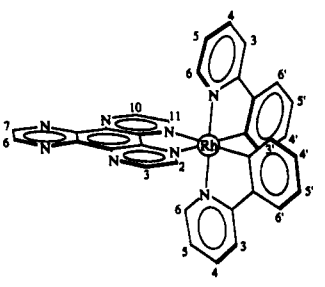

III

* Author to whom correspondence should be addressed.
† Director of Research at the National Fund for Scientific Research (Belgium).
⊕ Abstract published in *Advance ACS Abstracts*, October 15, 1993.

(1) Masschelein, A.; Kirsch-De Mesmaeker, A.; Verhoeven, C.; Nasielski-Hinkens, R. *Inorg. Chim. Acta* **1987**, *L13*, 129.
(2) Kirsch-De Mesmaeker, A.; Jacquet, L.; Masschelein, A.; Vanhecke, F.; Heremans, K. *Inorg. Chem.* **1989**, *28*, 2465.
(3) Vanhecke, F.; Heremans, K.; Kirsch-De Mesmaeker, A.; Jacquet, L.; Masschelein, A. *J. Raman Spectrosc.* **1989**, *20*, 617.
(4) Jacquet, L.; Kirsch-De Mesmaeker, A. *J. Chem. Soc., Faraday Trans.* **1992**, *88*, 2471.

0020-1669/93/1332-5239$04.00/0

scopic characteristics are reported and compared to previously published data[7-12] on $Rh(PPY)_2BPY^+$ and $Ir(PPY)_2BPY(/PHEN)^+$, which do not behave exactly like the TAP and HAT complexes.

The $Rh(PPY)_2BPY^+$ complex is indeed reported in the literature to luminesce at 77 K from a $^3\pi-\pi^*$ [7,8] excited state localized on the PPY, with some mixing with an ^{3}MLCT.[8] The $Ir(PPY)_2BPY^+$ differs from the corresponding rhodium complex by a dual emission at low temperature discussed as originating from two nonequilibrated ^{3}MLCT states, one toward a BPY and another toward a PPY ligand.[7-9]

The knowledge of the properties of the monomeric heteroleptic Rh and Ir unit with the HAT ligand described in this paper is of course essential for a further study of the polynuclear complexes built from these monometallic building blocks. Such polynuclear edifices can indeed be formed by the reaction of the Rh dichloro-bridged dimer with the monometallic Rh–HAT complex to form the bi- and trimetallic homonuclear complexes of Rh(III);[13] moreover, $Ru(BPY)_2HAT^{2+}$ and $[Ru(BPY)_2]_2HAT^{4+}$ can also react with the same Rh dichloro-bridged dimer to give rise to polymetallic heteronuclear complexes of Rh and Ru.[13]

Experimental Section

Syntheses and Characterizations. The heteroleptic complexes $Rh(PPY)_2HAT^+(PF_6^-)$, $Rh(PPY)_2TAP^+(PF_6^-)$, and $Ir(PPY)_2HAT^+(PF_6^-)$ are prepared from the appropriate dichloro-bridged dimer $[Rh(PPY)_2Cl]_2$ or $[Ir(PPY)_2Cl]_2$ reacting with TAP or HAT. The three corresponding chloride salts of the complexes are prepared by exchanging the PF_6^- with an anion exchanger (DEAE-A50, Pharmacia). The method applied to prepare $[Rh(PPY)_2Cl]_2$ has been slightly modified with respect to the literature.[14] The $[Ir(PPY)_2Cl]_2$ dimer was provided by R. J. Watts, University of California, Santa Barbara, CA. The purity of the complexes is tested by HPLC which allows the detection of a few percents of complex impurity. HPLC conditions: column, Bondapak C-18, Millipore Waters; gradient program, 0–100% methanol/water pH 2.5 (H_3PO_4) from 5 to 15 min; detection, 220–500 nm.

$Rh(PPY)_2TAP^+(PF_6^-$ or $Cl^-)$. $[Rh(PPY)_2Cl]_2$ (47 mg; 0.05 mmol) and TAP (18 mg; 0.1 mmol) are refluxed together in a dichloromethane/methanol mixture (1:1; 30 mL) for 3 h. The solvent is evaporated, and the remaining solid is dissolved in a minimum amount of water. On addition of a saturated aqueous solution of KPF_6 the complex (yellow) precipitates (0.04 mmol; yield = 80%). ES(electrospray) MS (m/z observed for the largest isotopic peaks and calculated values in parentheses): cone voltage = 45 V, 593.0, 100% (593.09), $[M - Cl^-]^+$.

$Rh(PPY)_2HAT^+(PF_6^-$ or $Cl^-)$. $[Rh(PPY)_2Cl]_2$ (47 mg; 0.05 mmol) in dichloromethane (15 ml) is added dropwise to a refluxing suspension of HAT (35 mg; 0.15 mmol) in 15 mL of a dichloromethane/methanol (1:1) mixture. After 4 h, the solvent is evaporated, 10 mL of water is added to the solid and the remaining nondissolving HAT ligand is filtered off. The dissolved complex is loaded on a SEPHADEX C-25 column (Pharmacia), eluted by a 0.1 M NaCl solution. The fraction containing the complex with NaCl is evaporated, and the compound is extracted with a minimum amount of methanol; the nondissolving salt is filtered off and the methanolic solution evaporated to dryness. The residue is dissolved in a minimum amount of water and the complex precipitated by addition of a saturated solution of KPF_6 in water: 32 mg (0.04 mmol) of a yellow precipitate of $Rh(PPY)_2HAT^+(PF_6^-)$ is collected. Yield: 80%. ESMS (m/z observed for the largest isotopic peaks and calculated values in parentheses): cone voltage = 45 V, 645.26, 100% (645.10), $[M - Cl^-]^+$; cone voltage = 100 V, 645.32, 25% $[M - Cl^-]^+$, 411.30, 100% (411.04), $[M - Cl^- - HAT]^+$.

$Ir(PPY)_2HAT^+(PF_6^-$ or $Cl^-)$. The iridium complex is synthesized and purified according to the same procedure as for the $Rh(PPY)_2HAT^+(PF_6^-)$, using $[Ir(PPY)_2Cl]_2$ (44 mg; 0.05 mmol) instead of $[Rh(PPY)_2Cl]_2$: 35 mg (0.04 mmol) of the red-orange colored $Ir(PPY)_2HAT^+(PF_6^-)$ is isolated. Yield: 80%. ESMS (m/z observed for the largest isotopic peaks and calculated values in parentheses): cone voltage = 45 V, 735.24, 100% (735.16), $[M - Cl^-]^+$; cone voltage = 130 V, 735.43, 15% $[M - Cl^-]^+$, 501.27, 100% (501.09), $[M - Cl^- - HAT]^+$.

Equipment. Absorption spectra are recorded on a Hewlett Packard HP 8452A UV–visible diode array spectrophotometer, and emission spectra, with a modified Applied Photophysics Laser Kinetic spectrometer, equipped with a Hamamatsu R928 photomultiplier tube (PMT). Correction of the emission for the response of the PMT is achieved on the basis of a standardized emission spectrum of a 200-W quartz–halogen lamp (Model M-217/220A from Optotronics Laboratories). Excitation is performed with a 300-W xenon arc lamp (Optical Radiation Corp., XM 300-5).

Emission lifetimes are measured in the Laser Kinetic spectrometer already mentioned above equipped with a Hamamatsu R 928 PMT, by exciting the samples at 337 nm with a Molectron UV-24 (8-ns pulse width) nitrogen laser. Signals are recorded with a digital oscilloscope (HP 54200 A), connected through an IEEE 488 interface to an HP 9816 S computer, and are averaged over at least 16 shots; base-line corrections are also introduced. Kinetic analyses of the traces are performed by nonlinear least-squares regression using a modified Marcquardt algorithm.[15] An Oxford Instruments DN 1704 nitrogen cryostat controlled by an Oxford Instruments Intelligent Temperature Controller (ITC 4) is used for the low-temperature emission lifetimes and luminescence spectra.

The transient absorption spectra of the Rh excited complexes are obtained by excitation of the samples at 355 nm with a pulsed neodynium–YAG laser (Continuum NY 61-10); the detection is performed with the Applied Photophysics Laser Kinetic Spectrometer described previously.[4] In cyclic voltammetry, the potential of the working electrode (platinum disc electrode; approximate area; 20 mm^2) is controlled by a homemade potentiostat and measured versus a saturated calomel electrode (Radiometer K701) with a large surface area Pt grid as counter-electrode.

NMR spectra are recorded on a Bruker Cryospec WM 250 MHz.

Chemicals. Acetonitrile (Aldrich, 99.8%), for cyclic voltammetry, is refluxed for several hours over P_2O_5, distilled, and refluxed again over CaH_2, just before the last distillation prior to the electrochemical measurements. The supporting electrolyte tetrabutylammonium hexafluorophosphate (TBAH) (Fluka puriss) is vacuum dried at 60° C for 1 day. Acetonitrile (Aldrich, spectroscopic grade) is used without further purification for the absorption and emission measurements.

Results

Characterization by NMR Spectroscopy. As the ligand PPY is nonsymmetric, the resulting ortho-metalated complexes with two PPY and one HAT or one TAP ligand can give rise to different structural isomers depending on the relative positions of the Rh–C bonds. As the ^{1}H NMR spectra show three different protons for the TAP or HAT ligands and eight for the PPY ligands (Table I), this indicates the existence of a C_2 axis bisecting the ligand TAP or HAT. The isomers have thus their Rh–C bonds either in the cis position or in the trans position. NOE experiments[16] on $Rh(PPY)_2BPY^+$ and XR data for complexes of Pt(II) with PPY and for complexes of Rh(III) with azoarenes[17,18a] and with one diimine and other ortho-metalating ligands[18b] have demonstrated that the two metal–C bonds are always in the cis position in this type of ortho-metalated complexes. Consequently by

(5) Sprouse, S.; King, K. A.; Spellane, P. J.; Watts, R. J. *J. Am. Chem. Soc.* **1984**, *106*, 6647.
(6) King, K. A.; Spellane, P. J.; Watts, R. J. *J. Am. Chem. Soc.* **1985**, *107*, 1431.
(7) Ohsawa, Y.; Sprouse, S.; King, K. A.; DeArmond, M. K.; Hanck, K. W.; Watts, R. J. *J. Phys. Chem.* **1987**, *91*, 1047.
(8) Maestri, M.; Sandrini, D.; Balzani, V.; Mäder, U.; von Zelewsky, A. *Inorg. Chem.* **1987**, *26*, 1323.
(9) (a) Wilde, A. P.; Watts, R. J. *J. Phys. Chem.* **1991**, *95*, 622. (b) Wilde, A. P.; King, K. A.; Watts, R. J. *J. Phys. Chem.* **1991**, *95*, 629.
(10) Sandrini, D.; Maestri, M.; Balzani, V.; Mäder, U.; von Zelewsky, A. *Inorg. Chem.* **1988**, *27*, 2640.
(11) Zilian, A.; Mäder, U.; von Zelewsky, A.; Güdel, H. *J. Am. Chem. Soc.* **1989**, *111*, 3855.
(12) Frei, G.; Zilian, A.; Raselli, A.; Güdel, H. U.; Bürgi, H.-B. *Inorg. Chem.* **1992**, *31*, 4766.
(13) Didier, P.; Jacquet, L.; Kirsch-De Mesmaeker, A.; Hueber, R.; van Dorsselaer, A. *Inorg. Chem.* **1992**, *31*, 4803.
(14) Nonoyama, M.; Yamasaki, K. *Inorg. Nucl. Chem. Lett.* **1971**, *7*, 943.
(15) Demas, J. N. in *Excited State Lifetime Measurement*; Academic Press: New York, 1983.
(16) Mäder, U.; Jenny, T.; van Zelewsky, A. *Helv. Chim. Acta* **1986**, *69*, 1085.
(17) Hoare, R. J.; Mills, O. S. *J. Chem. Soc., Dalton Trans.* **1972**, 2138.
(18) (a) Craig, R. M.; Knox, G. R.; Pauson, P. L.; Hoare, R. J.; Milss, O. S. *J. Chem. Soc., chem. Commun.* **1971**, 168. (b) Maeder, U.; von Zelewsky A.; Stoekli-Evans, H. *Helv. Chim. Acta.* **1992**, *75*, 1320.

Table I. NMR Data for the Rh(III) and Ir(III) Complexes in CD_3CN

PPY-[a]		TAP[a]
$Rh(PPY)_2TAP^+$		
H(3): 8.07 (d, J = 8.1)	H(6'): 7.89 (d, J = 8.9)	H(2) + H(7): 9.22 (d, J = 2.3)
H(4): 7.88 (dd)	H(5'): 7.17 (dd)	H(9) + H(10): 8.59 (s)
H(6): 7.44 (d, J = 5.5)	H(4'): 7.04 (dd)	H(3) + H(6): 8.32 (d, J = 2.3)
H(5): 6.92 (dd)	H(3'): 6.37 (d, J = 7.6)	
$Rh(PPY)_2HAT^+$		
PPY-		HAT
H(3): 8.10 (d, J = 8.1)	H(6'): 7.89 (d, J = 8.9)	H(3) + H(10): 9.35 (d, J = 2.3)
H(4): 7.89 (dd)	H(5'): 7.19 (dd)	H(6) + H(7): 9.37 (s)
H(6): 7.54 (d, J = 5.8)	H(4'): 7.06 (dd)	H(2) + H(11): 8.43 (d, J = 2.5)
H(5): 6.94 (dd)	H(3'): 6.38 (d, J = 7.6)	
$Ir(PPY)_2HAT^+$		
PPY-		HAT
H(3): 8.09 (d, J = 8.1)	H(6'): 7.87 (d, J = 7.8)	H(3) + H(10): 9.32 (d, J = 2.5)
H(4): 7.83 (dd)	H(5'): 7.13 (dd)	H(6) + H(7): 9.39 (s)
H(6): 7.55 (d, J = 5.8)	H(4'): 7.01 (dd)	H(2) + H(11): 8.42 (d, J = 2.5)
H(5): 6.89 (dd)	H(3'): 6.35 (d, J = 7.9)	

[a] Chemical shifts in ppm; multiplicity and coupling constants in Hz. For the numbering of the protons, see Figure 1. The spectra have been recorded in standard conditions with a digital resolution of 0.4 Hz/point so that only the coupling constants for the ortho positions are given in the table.

extrapolation, we attribute the isomer with a C_2 symmetry, which we have isolated from the synthesis, to that with its metal–Carbon bonds in a cis position. In the $Rh(PPY)_2TAP^+$, for example, the C_2 symmetry axis makes the TAP's protons H(2), H(3), and H(10) equivalent to the protons H(7), H(6), and H(9) respectively (see II). A 2D-COSY ^1H–^1H spectrum of the $Rh(PPY)_2TAP^+$ (Figure 1a) and a comparison with the spectra of $Rh(PPY)_2BPY^+$ [16] studied in the literature, allow the assignment of all the chemical shifts (Table I). The TAP protons occur at lower field than those of the PPY owing to the π-deficient character of this ligand. The protons H(9) and H(10) appear as a singlet at 8.59 ppm and the protons H(3) and H(6) correspond to the most shielded doublet, as observed previously with the other TAP complexes,[19] because of their shielding by the electronic ring current of the adjacent PPY ligands. The most unshielded doublet is then attributed to the protons H(2) and H(7).

In the phenylic cycle of the ligand PPY,[16] the proton in ortho position to the Rh–C bond [H(3')] is the most shielded doublet again because of the effect of the ring current of the adjacent PPY. The second doublet at 7.89 ppm is then assigned to H(6'). The assignments for H(4') and H(5') are then straightforward. In the pyridinic cycle of the ligand PPY, the assignment of the different protons is also quite similar to that for the $Rh(PPY)_2BPY^+$.[16] The protons assignment for the two other analogous complexes has been performed by comparison with the $Rh(PPY)_2TAP^+$ (Table I and Figure 1b for $Ir(PPY)_2HAT^+$).

Electrochemistry. The electrochemical data for the TAP and HAT complexes are collected in Table II, together with the data for the dichloro-bridged dimers[7] and for the monometallic BPY complex[7] for comparison.

The electrochemical behavior is similar for the TAP and HAT complexes. These latter show a comparable reduction pattern, with two reversible waves observed in the potential scale accessible by cyclic voltammetry in acetonitrile. In oxidation, the waves for the Rh complexes are completely irreversible, as indicated by the absence of reduction of the oxidized compound during the reverse scan of the electrode potential. For $Ir(PPY)_2HAT^+$, on the other hand, the oxidation wave becomes quasi-reversible at 0.1 V/s with a ratio of the oxidation and reduction peaks close to unity.

Absorption and Emission Spectroscopy. The absorption spectra in MeCN, for $Rh(PPY)_2TAP^+$, $Rh(PPY)_2HAT^+$, and $Ir(PPY)_2HAT^+$ are shown in Figure 2; the previously published absorption of $Rh(PPY)_2BPY^+$ is included for purposes of comparison. Peak positions and extinction coefficients from these spectra are compiled in Table III. The values of the extinction coefficients for the bands at ≈350 nm (Rh complexes) and ≈370 nm (Ir complexes) are compatible with those expected for charge transfer transitions. For all of the complexes, weak absorption tails which extend out into the visible region of the spectrum (500 nm for the Ir complex) give rise to the yellowish and red-orange colours of the Rh and the Ir compounds, respectively.

Both $Rh(PPY)_2TAP^+$ and $Rh(PPY)_2HAT^+$ show structureless emission spectra at room temperature as well as in frozen glass matrices (Figure 2). Large blue shifts in the emission maxima are evident on cooling from room temperature to 77 K. The emission characteristics of $Ir(PPY)_2HAT^+$ are slightly different: the hypsochromic shift at 77 K is accompanied by a broadening of the spectrum in EtOH/MeOH (4:1), and this broadening is replaced by two distinct maxima separated by ≈ 550 cm^{-1} in a propionitrile/butyronitrile (4:1) glass. In contrast, the emission spectrum of $Rh(PPY)_2(BPY)^+$ (included in Figure 2 for comparison) is highly structured at low temperatures and the peak maxima shift very little between room temperature and 77 K: this emission has been assigned to a $^3\pi$–π^* excited state localized upon the PPY ligand.[7,8] Emission maxima in several different solvents at room temperature and at 77 K are compiled in Table IV.

Pulsed laser excitation of the Rh–TAP and –HAT complexes at either 77 K or room temperature at 337 nm leads to luminescence which is characterized by a single exponential decay with lifetimes compiled in Table IV. Emission lifetimes in water are too short to monitor with the laser system described in this paper; it is well-known that the OH vibrations of the solvent are efficient acceptors which promote rapid nonradiative decay of excited solutes.[20] The emission lifetime of $Rh(PPY)_2(BPY)^+$ is also too short to measure at room temperature, but in this case, similar conclusions have been reached for all solvents for which the measurement was attempted. The excited state lifetime of $Ir(PPY)_2HAT^+$ in room temperature fluid solutions is also too short to measure with the present apparatus. At 77 K, the

(19) Kirsch-De Mesmaeker, A.; Nasielski-Hinkens, R.; Maetens, D.; Pauwels, D.; Nasielski, J. *Inorg. Chem.* **1984**, *23*, 377.

(20) Meyer, T. J. *Pure Appl. Chem.* **1986**, *58*, 1193.

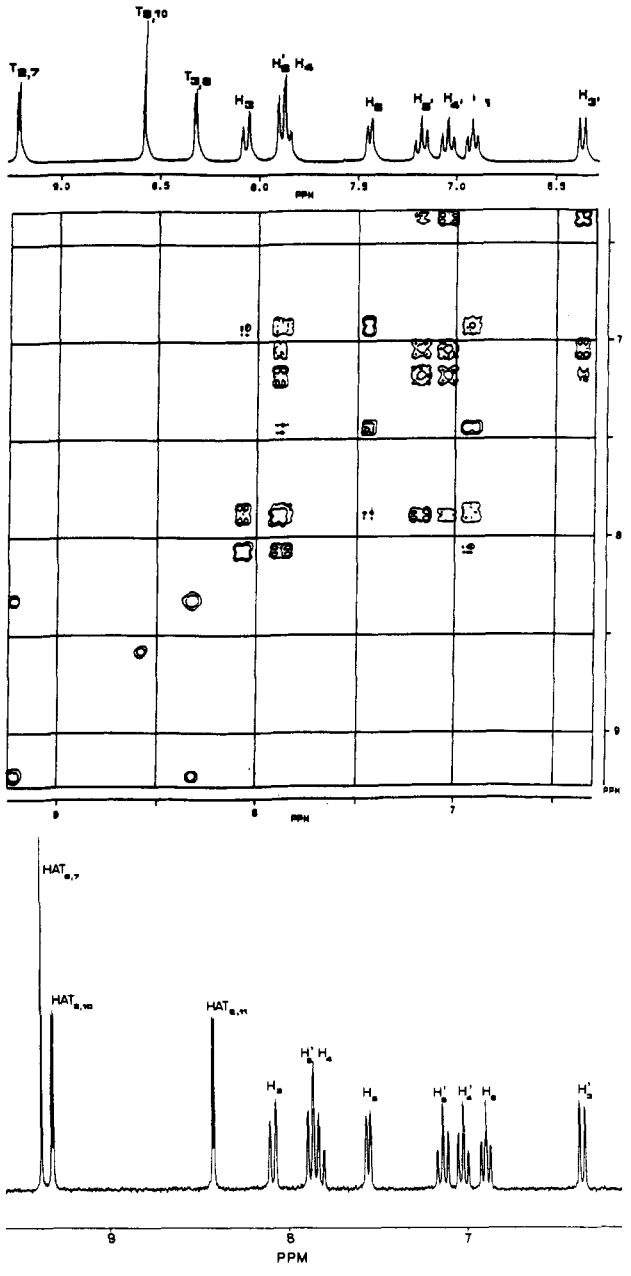

Figure 1. Top: (A) 2D COSY ^{1}H-^{1}H spectrum of $Rh(PPY)_2TAP^+$ in CD_3CN. Bottom: (B) ^{1}H NMR spectrum of $Ir(PPY)_2HAT^+$ in CD_3CN.

luminescence of this complex does not decay via single exponential kinetics, and biexponential regression analysis leads to a much better fitting of the luminescence decay curves. The luminescence lifetimes and relative contribution of each of the two components of a biexponential analysis are collected in Table IV. These data indicate that the contribution of each of the two decay components depends upon the wavelength of the emission.

The differential transient absorption spectra recorded after a laser pulse at 355 nm are shown in Figure 3 for $Rh(PPY)_2TAP^+$ and $Rh(PPY)_2HAT^+$ in acetonitrile at room temperature; the transient absorption for $Ir(PPY)_2HAT^+$ could not be measured due to its too short excited state lifetime in fluid solutions. The decays of the transient absorption signals were found to have decay constants similar to those for the luminescence in acetonitrile, indicating that the transient spectra are due to absorption of the excited state. The negative signal from *ca.* 600 nm in the transient absorption spectra originates from interference due to emission.

Table II. Electrochemical Data for the Rh(III) and Ir(III) Complexes

complex[a]	E_{red1}	E_{red2}	E^*_{red1}	E_{ox}	E^*_{ox}
$[Rh(PPY)_2Cl]_2$	−1.86 (ir)			+1.53 (ir)	
	−2.04 (ir)[b]			+1.26 (ir)[b]	
$Rh(PPY)_2BPY^+$	−1.49 (r)		+1.10	+1.42 (ir)	−1.18
	−1.48 (r)[c]	−2.13 (r)[c]		+1.56 (ir)[b]	
$Rh(PPY)_2TAP^+$	−0.95 (r)	−1.60 (r)	+0.86	+1.65 (ir)	−0.26
$Rh(PPY)_2HAT^+$	−0.88 (r)	−1.49 (r)	+0.93	+1.59 (ir)	−0.25
$[Ir(PPY)_2Cl]_2$	−2.04 (ir)[b]			+0.97 (r)[b]	
$Ir(PPY)_2BPY^+$	−1.41 (r)[c]	−2.06 (r)[c]		+1.22 (r)[b]	
$Ir(PPY)_2HAT^+$	−0.75 (r)	−1.37 (r)	+0.86	+1.43 (110 mV)	−0.21
				+1.42 (190 mV)[d]	

[a] Reduction and oxidation potentials in V/SCE determined by cyclic voltammetry at a Pt electrode, in CH_3CN containing 0.1 M $But_4N^+PF_6^-$; scan rate = 0.1 V/s; r = reversible and ir = irreversible wave; in parentheses are given the values of ΔE_{peak} in mV. E^*_{red1} and E^*_{ox} = reduction and oxidation potentials in the excited state. [b] In CH_3CN, at −40 °C; scan rate = 1 V/s.[7] [c] In DMF, at −54 °C, scan rate = 1 V/s[7]; a third and fourth reduction wave are still observed. [d] In CH_3CN at 0.01 V/s.

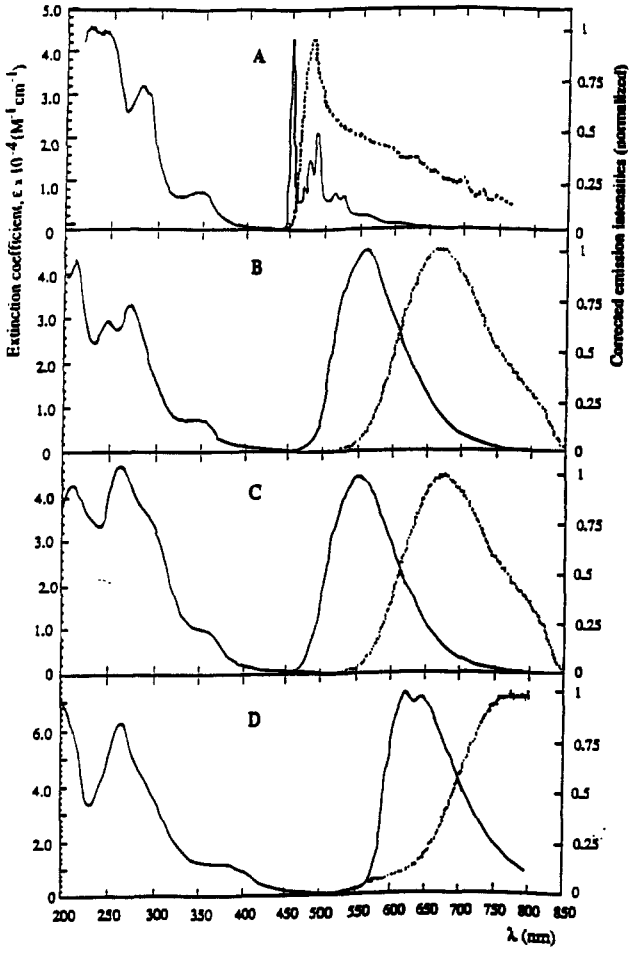

Figure 2. Absorption and emission spectra of the ortho-metalated complexes. Absorption and corrected emission in CH_3CN at 298 K (---) and at 77K in an EtOH/MeOH 4:1 glass for A,B,C and in a propionitrile/butyronitrile 4:1 glass for D(—). A ≡ $Rh(PPY)_2BPY^+$, B ≡ $Rh(PPY)_2TAP^+$, C ≡ $Rh(PPY)_2HAT^+$, and D ≡ $Ir(PPY)_2HAT^+$.

Discussion

Electrochemistry. As mentioned above, $Rh(PPY)_2TAP^+$ and $Rh(PPY)_2HAT^+$ both show two reversible reduction waves in the potential range accessible in acetonitrile at room temperature. These reductions occur at potentials slightly less negative with HAT than with the TAP ligand, in accordance with the more π-deficient character of HAT. Moreover, as these two ligands are far better π acceptors than the BPY or the PPY ligands, a more negative potential is needed for the reduction of $Rh(PPY)_2(BPY)^+$. Similar reduction behavior is observed for the Ir–HAT

Table III. Absorption Data[a] for the Rh(III) and Ir(III) Complexes

complex	CH_3CN	H_2O
$Rh(PPY)_2BPY^+$	241 [4.53]	242, 256, 296
	256 [4.48]	306, 362
	296 [3.20]	
	305 [sh]	
	364 [0.73]	
$Rh(PPY)_2TAP^+$	229 [4.28]	228 [7.1]
	263 [2.93]	260 [4.2]
	284 [3.19]	286 [4.9]
	352 [0.73]	350 [1.1]
$Rh(PPY)_2HAT^+$	213 [4.32]	214, 266 [4.65]
	264 [4.65]	290 (sh)
	290 (sh)	354 [0.92]
	354 [0.92] (sh)	
$Ir(PPY)_2BPY^+$		252 [3.6],[b] 265
		310, 375 [0.75]
		410 (sh)
		465 [0.06]
$Ir(PPY)_2HAT^+$	264 [6.38]	264 [4.5]
	288 (sh)	376 [0.7]
	370 [1.15]	

[a] Maxima of absorption; in brackets are given the molar absorption coefficients, $\epsilon \times 10^{-4}$ M^{-1} cm^{-1}; sh = shoulder. [b] In MeOH.[7]

Table IV

(a) Emission Data[a]

	298 K λ_{max}^{em}, nm [τ, ns]		77 K λ_{max}^{em}, nm [τ, μs]
complex	CH_3CN	prop carb	EtOH/MeOH 4:1
$Rh(PPY)_2BPY^+$	480 [<10]		454, 471, 479, 489, 506, 516, 528 [181]
$Rh(PPY)_2TAP^+$	668 [175]	635 [160]	553 [10.5]
$Rh(PPY)_2HAT^+$[f]	675 [90]	660 [120]	584 [7.4]
$Ir(PPY)_2BPY^+$	[337][d]		520,[b] 550[b] [4.5, 7.0][b]
$Ir(PPY)_2HAT^+$	>770 [<10]	730 [<10]	650[c] [see part b]

(b) Lifetime Data

		77 K[e]			
		EtOH/MeOH 4:1		propionitrile/butyronitrile 4:1	
complex	λ_{max}^{em}, nm	τ_1, μs	τ_2, μs	τ_1, μs	τ_2, μs
$Ir(PPY)_2HAT^+$	620	0.55 (45%)	1.31 (55%)		
	650	0.45 (60%)	1.19 (40%)		
	615			1.91 (40%)	3.14 (60%)
	640			1.49 (50%)	2.91 (50%)

[a] Corrected for the photomultiplier response. [b] Emission data 50 ns after an excitation with a laser pulse at 470 nm; decay analyzed according to a biexponential regression.[7] [c] Broad spectrum as compared to a room-temperature spectrum. [d] Reference 7. [e] Luminescence decay analyzed according to a biexponential regression; in parentheses, the percent contribution for each component. This analysis leads to correct values of the lifetimes (τ_1, τ_2) if the values are different by at least a factor of 4. This is not the case for these complexes; therefore, τ_1 and τ_2 present errors probably on the order of 30%. [f] Its emission maximum in water appears at 690 nm, with a lifetime shorter than 10 ns.

complex as seen for the Rh–HAT compound, with a slight positive shift of the reduction potential for the Ir species relative to Rh.

Different arguments suggest that the two reduction waves correspond to a successive addition of electrons *to the same* TAP or HAT ligand: (i) for the $Rh(PPY)_2(BPY)^+$ and $Rh(PPY)_2(PHEN)^+$,[7,8] the fact that only one reduction wave associated with the addition of one electron on BPY or PHEN, respectively, is observed in the accessible potential range at room temperature; (ii) the fact that the *two* waves observed with $Rh(PPY)_2HAT^+$ are anodically shifted as compared to those associated to the TAP compound; (iii) the fact that the PPY reduction in $Rh(PPY)_2(BPY)^+$ is observed only at potentials more negative than −2.4 V in *N*,*N*-dimethylformamide at −54 °C.[7]

Concerning the oxidation pathway, the wave is totally irreversible for the Rh–HAT and –TAP complexes whereas the oxidation wave becomes quasi-reversible for $Ir(PPY)_2HAT^+$ at high scan rates. As in the Rh–HAT and –TAP complexes, the oxidation wave of $Rh(PPY)_2(BPY)^+$ is irreversible, but a reversible oxidation wave has been reported for $Ir(PPY)_2(BPY)^+$. The orbital origin of the electron removed by oxidation is quite relevant to characterization of the nature of the spectroscopic charge transfer processes seen in these complexes, and MLCT from Ir(III) to the ligand, believed to give rise to the lowest excited state in $Ir(PPY)_2(BPY)^+$, is consistent with metal-centered oxidation behavior in cyclic voltammetry. On the other hand, the cyclic voltammetric results described above for the Ir–HAT complex suggest that the oxidation might not be the result of loss of a dπ electron from the metal center. This point will be discussed further when the spectroscopic results of this study are considered below.

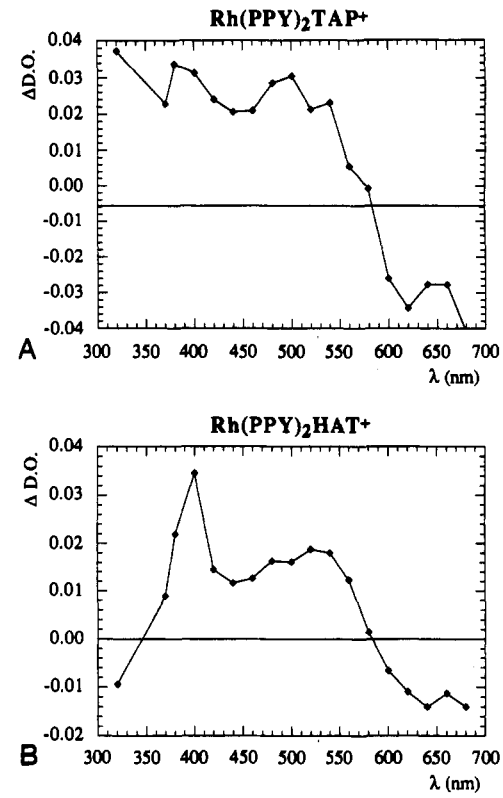

Figure 3. Differential transient absorption spectra: (A): $Rh(PPY)_2TAP^+$ and (B) $Rh(PPY)_2HAT^+$ in CH_3CN, a few ns after the laser pulse, $\lambda_{excitation}$ = 355 nm.

The π-deficient character of the HAT ligand relative to BPY is reflected in the positions of the oxidation waves of $Ir(PPY)_2HAT^+$ and $Rh(PPY)_2HAT^+$, which occur at more positive potentials than those seen in $Ir(PPY)_2BPY^+$ and $Rh(PPY)_2(BPY)^+$. It is also noted that the difference between the oxidation waves in the Ir– and Rh–HAT complexes is somewhat smaller than the difference in the Ir–BPY and Rh–BPY oxidation waves. This may also be indicative of substantial variations in the origin of the electron which is removed in oxidation of the BPY complexes compared to the HAT complexes.

Redox Potentials in the Excited State. Estimated oxidation and reduction potentials for each complex in the excited state are compiled in Table II. In these approximations, the excited state energies have been taken as the Franck–Condon peak maxima from the emission spectra, and ground state oxidation potentials are taken as the oxidation peak potentials of the irreversible waves in cyclic voltammetry. The Rh–HAT and –TAP complexes are more oxidizing in the ground state than the –BPY complex, but less so in the excited state. This is largely due to the lower excited state energies of the –HAT and –TAP complexes as compared to the BPY complex. It is also observed that the Rh–HAT and –TAP complexes are far less reducing in their excited states as compared to the –BPY complex. Although this is consistent with

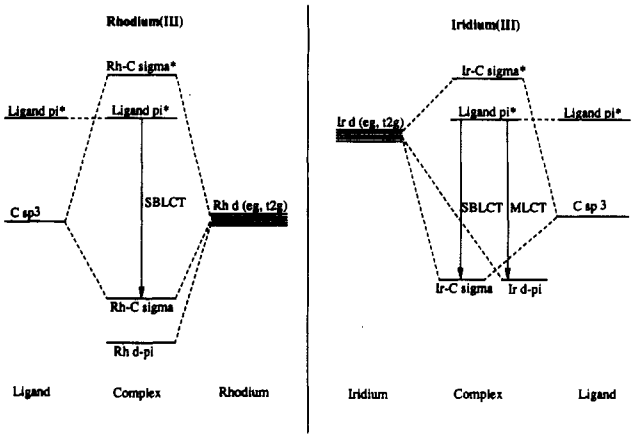

Figure 4. Qualitative molecular orbital diagram and resulting transitions for $Rh(PPY)_2HAT^+$ and $Ir(PPY)_2HAT^+$.

the ground-state behavior associated with the strong π-acceptor nature of HAT and TAP, the poor excited-state reducing character is further enhanced by the low energies of the Rh–HAT and –TAP excited states.

Absorption Spectroscopy and Electrochemical Data. Comparison of the UV-visible absorption spectra of the Rh–HAT and –TAP complexes with those of the HAT and TAP ligands indicate that the intense absorption bands below 300 nm can be assigned to ligand-centered (LC) or π–π^* transitions. Assignment of the absorption bands at longer wavelengths is, however, far more complicated. Since metal-centered (d–d) transitions are unlikely at low energies with the strong-field PPY ligands,[7,10] charge-transfer transitions are likely to give rise to the lower energy bands. For $Rh(PPY)_2BPY^+$ the band at 364 nm had first been assigned to a Rh–BPY charge transfer (CT), in agreement with the electrochemical behavior.[16] However assignment of this band to a Rh–PPY CT was supported by the finding of similar bands in $[Rh(PPY)_2Cl]_2$, $[Ir(PPY)_2Cl]_2$, and $Pt(PPY)_2$ where BPY is not present.[8,18b] This argument is also valid for the Rh–TAP and –HAT complexes as they show a CT band in the same wavelength region. However, as for the Rh–BPY complex, the electrochemical data in reduction also indicate an electron transfer to the diimine ligand. The electrochemical behavior in oxidation leads moreover to further information concerning the nature of these CT bands. Well-known MLCT behavior in complexes of HAT, TAP, and BPY with metals such as Ru(II) is associated with the reversibility of the oxidation wave, corresponding to the abstraction of one electron from the metal centered dπ orbital of the complex. Moreover, for the Rh–BPY, –TAP, and –HAT complexes as outlined above, the low-energy absorption band is assigned to MLCT transitions, although no reversibility is observed for the oxidation wave. On the other hand, oxidation of Rh(III) is expected to occur at very high positive potentials, probably more positive than those determined for the oxidation of HAT–Ru(II) complexes (>2.1 V/SCE), which is not what is actually observed for these Rh(III) complexes. Therefore other types of charge-transfer behavior should be seriously considered.

Of particular concern is a type of charge transfer originating from the potentially highly covalent nature of Rh-C bonds in complexes such as $Rh(PPY)_2(HAT)^+$, $Rh(PPY)_2(TAP)^+$, and $Rh(PPY)_2(BPY)^+$. Where covalency becomes important, the nature of the HOMO in these metal complexes may result from a strong admixture of a σ-bonding ligand orbital and a dσ (e_g) metal orbital. A qualitative molecular orbital diagram which is useful in describing the effects of this type of covalency and the resulting transitions is illustrated in Figure 4. A similar diagram has been utilized in interpretations of spectral transitions in complexes containing highly covalent Re(I)–Ge and Re(I)–Sn[21] bonds as well as in descriptions of transitions in Rh(III)–Si and Ir(III)–Si bonded species.[22] In this diagram, participation of the metal in the HOMO is due to the σ-acceptor nature of the metal e_g orbitals. The molecular orbitals resulting from the π-donor character of the metal t_{2g} orbitals are probably at lower energy than the HOMO in cases where high covalency occurs. If such is the case, the electrons which occupy the HOMO may be viewed as originating from the carbanion formed by loss of a proton as the metal–carbon bond is formed. Low-energy charge-transfer transitions may then occur as a result of promotion of an electron from the metal–ligand σ-bonding orbital to the π^*-acceptor orbital of a ligand. These transitions, which are denoted as σ-bond-to-ligand charge-transfer (SBLCT), lead to substantial charge separation, just as MLCT transitions do, but are quite distinct from MLCT in several regards.

As indicated above, the electron which is promoted in these transitions does not originate from a dπ metal-centered orbital as in MLCT, but rather from a Lσ–dσ bonding orbital in which the metal acts as an acceptor and the ligand as a donor. As a result, the transition does not give rise to a formally oxidized metal center, as in MLCT, but rather to loss of a bonding electron with substantial disruption of the M–C bonding framework. One might therefore anticipate a high level of distortion in SBLCT excited states as well as possible photochemical activity in which the metal–carbon bond is cleaved due to loss of a bonding electron. This description of SBLCT contrasts with formulation of MLCT as an oxidized metal center coupled with a ligand radical anion which is formed from the ground state without any major influence upon the metal-ligand bonding framework. These two formulations are depicted schematically here in the case of an electron transfer to the diimine ligand:

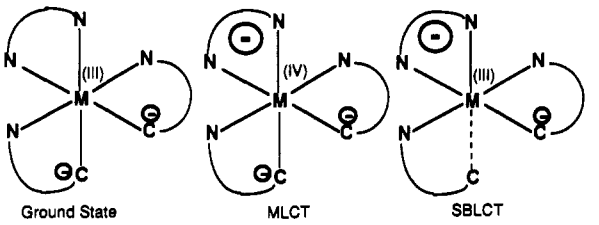

The irreversible oxidation wave observed in the Rh–HAT, –TAP, or $-BPY$[8,16,18b] complexes suggests that the electron removed in this process originates from a Lσ–dσ bonding orbital; irreversibility in this case is expected to originate from subsequent cleavage of the Rh–C bond. This formulation suggests that the absorption bands which peak at about 350–360 nm might be due to SBLCT transitions in which an electron is promoted from the Lσ–dσ bonding orbital (HOMO) to a π^* orbital of a ligand (LUMO). Although prior studies of $Rh(PPY)_2(BPY)^+$ [8,16,18b] indicate that absorption transitions in this region are due to MLCT, the similar redox behavior observed in cyclic voltammetry for that complex also suggests reformulation of the assignment to an SBLCT rather than an MLCT transition. These considerations however do not eliminate the uncertainty concerning the assignment of the LUMO to a π^* orbital of the diimine or PPY ligand, according to arguments in electrochemistry or absorption spectroscopy respectively. In contrat, the emission data for the Rh–TAP and –HAT complexes discussed below are in good agreement with the electrochemical data, indicating a charge transfer to the TAP or HAT ligand.

In the Ir–HAT complex, the low-energy absorption maximum is slightly red shifted (370 nm) relative to that for corresponding Rh–HAT species. This shift is consistent with increased

(21) Luong, J. C.; Faltynek, R. A.; Wrighton, M. S. *J. Am. Chem. Soc.* **1979**, *101*, 1597.
(22) Djurovich, P. I.; Safir, A.; Keder, N.; Watts, R. J. *Coord. Chem. Rev.* **1991**, *111*, 201.

ease of oxidation of Ir(III) relative to Rh(III), and may be attributed in general to the increased energy of the Ir 5d orbitals in comparison to the Rh 4d orbitals (see Figure 4). However, added complexity in the Ir case is evident experimentally in the quasi-reversibility of the oxidation wave of the Ir–HAT complex at rapid scan rates. This quasi-reversibility would indicate that, in the Ir complex, the Lσ–dσ orbital may be supplanted by the metal-centered dπ orbital as the HOMO. This dπ orbital moves indeed substantially higher in energy in Ir(III) relative to Rh-(III) complexes, due to the increased energy of the 5d orbital set in Ir (Figure 4). Thus this quasi-reversibility would suggest the presence of low-energy MLCT absorption bands mixed with SBLCT character, responsible for the absorption at 370 nm. As indeed indicated in Figure 4, the increased energy of the 5d orbital set would lead to less covalency of the Ir–C σ-bond, due to an increase in the energy difference between the Lσ and dσ orbital set and would give rise to a red shift of the SBLCT absorption transition relative to the one in the Rh complex, occurring in the same absorption range as the MLCT bands.

In contrast to this, the $Ir(PPY)_2(BPY)^+$ complex displays a fully reversible oxidation wave in cyclic voltammetry, suggesting that the prior assignment of its low-energy absorption to MLCT may be correct. This contrasting behavior of the Ir–HAT complex with the Ir–BPY complex is consistent with the enhanced π-acceptor character of HAT relative to BPY, which leads to a net stabilization of the dπ orbitals in Ir–HAT relative to the Ir–BPY complex. It appears that small energy changes such as these are sufficient to modify the delicate energy balance between the dπ and Lσ–dσ orbital sets in these species.

Excited State Absorption and Emission Spectroscopy. Due to conclusions drawn above regarding the low-energy absorption bands of the Rh–HAT and –TAP complexes, it is reasonable to consider an SBLCT assignment of the emission spectra for these species also. The emission in the red around 670–680 nm is consistent with a charge transfer to TAP or HAT, in accordance with the electrochemical data. The structureless character of their emission spectra at low temperatures suggests a highly distorted excited state, and the large red shift which occurs in the emissions in room-temperature fluid solutions indicates substantial reorganization following excitation in a fluid medium. These characteristics are certainly consistent with expectations for SBLCT excited states where substantial charge redistribution and weakening of the Rh–C bonds are expected to result in both a highly distorted excited state and disruption of the solvent sphere leading to solvent reorganization in fluid medium. Observation of excited state absorption characteristics consistent with a HAT or TAP radical anion[23] (Figure 3A,B) provide further support for a charge-transfer excited-state assignment with a transfer to the diimine ligand, although MLCT as well as SBLCT could be consistent with observation of the radical anion. The low-temperature emission lifetimes of these species (10.5, 7.4 μs) are substantially shorter than the lifetime reported for the ligand-localized (π–π^*) emission of $Rh(PPY)_2(BPY)^+$ (181 μs). Although this is consistent with a high degree of spin–orbit coupling in the Rh–HAT and –TAP species due to enhanced interaction of the Lσ–dσ electron (or dπ electron) over a Lπ electron with the heavy metal center, the comparison cannot be stated with confidence until radiative lifetimes from quantum yields data become available. Perhaps it is more relevant to note that the luminescence lifetimes of the Rh–HAT and –TAP complexes are around 100 ns in fluid solutions while the lifetime of the ligand-localized emission of the Rh–BPY complex is too short to measure. This behavior is consistent with many other examples of comparison of charge transfer and ligand-localized emission behavior in heavy metal d^6 complexes in low-temperature glasses and fluid solutions. While the measured lifetimes of the Rh–HAT and –TAP complexes, as well as the excited state absorption data, might be indicative of either SBLCT or MLCT behavior, the unstructured emission spectra at low temperatures are difficult to reconcile with the expectation of a relatively small distortion anticipated for MLCT excited states. These considerations lead to assignment of the Rh–HAT and –TAP emissions as SBLCT transitions.

The added complexity noted in the oxidative cyclic voltammetry of the Ir–HAT complex is also evident in its emission spectroscopy. The occurrence of two emissions at low temperatures as well as the emergence of two maxima in the emission when monitored in propionitrile/butyronitrile glasses at 77 K suggests that two closely spaced states may be responsible for the low-temperature emission. For the $Ir(PPY)_2(BPY)^+$, two luminescences had also been observed at 77 K and were attributed to two MLCT states, one with a CT toward the BPY and the other toward the PPY.[7,9] Such an attribution is not valid for the Ir–HAT complex. Indeed for a substitution of a BPY by a HAT ligand in the Ir compound, we expect (i) an important bathochromic shift of the Ir–HAT MLCT emission, due to the important stabilization of the ligand π^* orbital for the HAT as compared to the BPY, in accordance with the relative reduction potentials of these two complexes, and (ii) a slight hypsochromic shift of the Ir–PPY MLCT emission in the Ir–HAT complex, due to a stabilization of the dπ level in this complex compared to the one in the Ir–BPY compound. Experimentally, an important red shift of the emission band is indeed observed with the Ir–HAT complex. However the second emission at 77 K, which could originate from the Ir–PPY CT state according to this hypothesis, is not blue-shifted but is also red-shifted in the Ir–HAT as compared to the Ir–BPY compound. This behavior is actually consistent, as noted above from the discussion of the oxidations in cyclic voltammetry, with admixture of SBLCT and MLCT states, and it may be that this mixing results in two closely spaced states which are unequilibrated in low-temperature glasses. The lifetime data from double exponential analysis (Table IV) indicate that the lifetimes of the two components are quite similar and that the longer-lived component has slightly more intensity at shorter wavelengths while a slight predominance of the shorter component is noted at longer wavelengths. However the lifetime differences are much too subtle for an accurate determination of the two lifetimes. At the present time it is not possible to estimate the relative importance of specific site solvation effects versus intrinsic intramolecular energy transfer considerations stemming from the presence of closely spaced excited states, as possible origins of nonexponential decay in the complex. In fact, it is likely that the two phenomena may be strongly interdependent and that separation of a description into inner-sphere and outer-sphere effects will have little utility.

The large red-shift noted in the emission spectrum in fluid solutions (Figure 2) is a further indication of a large separation of charge in the excited state, which leads to substantial solvent reorganization in fluid solutions. While this as well as the low-temperature emission data is indicative of a charge-transfer excited state, it is perhaps most accurate at the present time to regard this emission as a result of a strong admixture of SBLCT and MLCT behavior.

Acknowledgment. P.D. and I.O. thank the NATO and the IRSIA for a fellowship. The Communauté Française de Belgique is also gratefully acknowledged for its financial support. The authors thank A. van Dorsselaer and E. Leize from the laboratory of mass spectrometry at the Université Louis Pasteur, Strasbourg, France, for the ESMS.

(23) Tan Sien Hee, L.; Kirsch-De Mesmaeker, A. To be submitted for publication. The absorption of the TAP radical anion can easily be recorded in a spectroelectrochemical cell. For the HAT radical anion however, it is difficult to observe its first absorption band due to the low solubility of this ligand in the organic solvents.